

行政院國家科學委員會專題研究計畫成果報告

高層建築受風載行為之減振控制及風洞試驗研究(II)

計畫編號：NSC 90-2211-E-032-011

執行期限：90年8月1日至91年7月31日

主持人：吳重成 淡江大學土木系

計畫參與人員：鄭良儀、黃正昌 淡江大學土木系研究生

中文摘要

本文以風洞試驗探討主動質塊驅動器(Active Mass Driver)應用於高層建築減振之可行性。使用之高層建築模型為多自由度之縮尺模型，於頂層樓裝置主動質塊驅動器，考慮在不同風攻角下之不同型態反應設計適當控制器以進行風洞試驗。本試驗結果顯示優越控制效能，證實所提出方法之可行性，本研究並為國內首次成功將主動控制應用在風洞實驗上之實例。

關鍵詞：高層建築、主動質塊驅動器、主動控制、風洞試驗

Abstract

Wind loading on the high-rise buildings is complicated in nature, especially when the across-wind motion caused by the aero-elastic vortex shedding effect is considered. In this paper, a 4 degree-of-freedom scaled (1:300) model of a high-rise building equipped with active mass driver (AMD) is constructed on a wind tunnel to experimentally verify the applicability of active control for wind-induced motion under varied attack angle of wind. A systematic system identification scheme simply based on the input/output relation is proposed for the construction of nominal systems. The control law is determined based on the Linear Quadratic Gaussian (LQG) theorem in which a dynamic output feedback equation with acceleration feedback is formed for practical implementation. The experimental results show that the performance of the active controller following the design process proposed is remarkable in reducing the responses of high-rise buildings under different attack angle of wind. Furthermore, despite that the nominal system contains system uncertainty, the performance of LQG control remains quite promising and robust.

Keywords: High-rise Building, Active Mass Driver System, Attack Angle, Active Control, Wind Tunnel Tests

I. Introduction

Recently in many urban areas where the space is highly restricted, the trend toward constructing higher buildings becomes gradually popular. The apparent changes in their structural properties are the elongation of natural period and the increase of susceptibility to wind excitation. Though the strength capacity of these buildings under wind excitation are adequate, the stiffness lessened might cause excessive displacements and accelerations on which building serviceability and comfort of occupants depend. In the last decade, many research and industrial efforts have demonstrated that structural active control is efficient in reducing the wind-induced motion of high-rise buildings [Housner et al(1994), Kobori et al (1998)]. Notably, most of them are accomplished through numerical simulation especially for the along-wind motion due to the simpler nature of along-wind loading. For high-rise buildings, the across-wind motion contains a significant vortex frequency, the so-called vortex shedding effect, which is termed aeroelasticity in wind engineering [Simiu and Scanlan (1986)]. The vortex shedding frequency is proportional to the incoming mean wind velocity. In general, the across-wind response caused by vortex shedding is much more detrimental in wind engineering because it is several times larger than the along-wind response simply caused by wind buffeting [Wu et al(2001)]. Due to such complexity of wind load and the possible aeroelasticity in site, the applicability of active control to high-rise building subjected to vortex shedding effect shall be investigated. In this paper, a feasible and reliable control design process through wind tunnel tests of a 4-degree-of-freedom scaled high-rise building model equipped with an active mass driver (AMD) system is proposed for active control application to wind-induced motion under varied wind attack angles from the along-wind to across-wind direction. The advanced control strategy, linear quadratic gaussian (LQG) method is used to construct active controllers with acceleration feedback. The promising performance and robustness of the active controller verified from the experiments demonstrate the feasibility of the design process proposed.

II. Experimental Setup

To realistically represent the high-rise building behavior, we constructed a scaled building model for experiments based on the wind-excited benchmark building proposed by the structural control committee in the 2nd World Conference on Structural Control [Yang and Wu et al (1998)]. This prototype building has 76 story units with a square cross-section. To account for the possible multiple mode responses, the 76-story prototype is condensed to a 4 degree-of-freedom shear type scaled model of which the responses of each DOF represents those of the 37, 58, 68 and 76 story unit of the prototype, respectively. According to the capability of the boundary layer wind tunnel, the resulting scaling factor in length, velocity, and density are 1:300, 1:6 and 1:1, respectively. By similarity, other factors can be calculated accordingly. As shown in Fig.1 (a) is the frame skeleton of the scaled building model. The completed model with exterior walls attached, as shown in Fig. 1 (b), has a total height of 102 cm and 16cm×16cm of cross-section, resulting in a height/width ratio of 6.4. The natural frequencies and damping ratios of the scaled model obtained from the preliminary system identification are 6.30, 31.34, 64.36, 132.64 Hz and 2.45%, 1.74%, 3.12%, 2.23%, respectively.

An active mass driver (AMD) system composed of a linear servo-motor and a moving mass is installed on the top floor, as shown in Fig. 2. The movement of the moving mass is controlled by a proportional-integral-derivative (PID) controller aiming to track the control command proportional to its absolute acceleration. An additional digital high-pass filter (cut-off at 2 Hz) is also implemented to filter out the low frequency components in the control command to avoid the excessive displacement of the moving mass. During experiments, seven response quantities of the building are recorded. They are the relative displacement w.r.t the ground and absolute accelerations at the 1st, 2nd and 4th DOF, and the absolute acceleration of the moving mass of AMD system, denoted as $x_1, x_2, x_4, \ddot{x}_1, \ddot{x}_2, \ddot{x}_4, \ddot{x}_{md}$, respectively. The feedback quantities during active control can be chosen from them and denoted as the measurement output \mathbf{y} . To simulate the mean wind velocity profile for the suburban area, an atmospheric boundary layer with a gradient height of 400 m and power law exponent equal to 0.23 is generated on the wind tunnel.

III. System Identification

Due to unavailability of wind force measurement in practice, the dynamics of overall system with the active device integrated is represented by the block diagram shown in Fig. 3(a). In Fig. 3(a), the inputs of the overall system are expressed as the control command U and the fictitious excitation W assumed to be white noise, while the output is the so-called control output vector \mathbf{z} , which is composed of the

recorded building responses (7 quantities) and the filtered accelerations (3 quantities) via a high-pass filter. The inclusion of the filtered accelerations is for modulating the high frequency components when active control is employed. In this overall system, by assuming U and W be two independent inputs, the process of the input/output relation is divided into two cases represented by the solid and dashed borders in Fig. 3(a), leading to a simplified system block diagram in Laplace (Frequency) domain as shown in Fig. 3(b). During the tests, the wind blow direction is considered for the possible vortex shedding effect. The configuration of wind attack angle and the measuring direction of the building responses are shown in Fig. 4. In Case 1 where the wind disturbance is absent ($W=0$), a banded white noise of control command U is fed into the 2-Hz digital high-pass filter to obtain the filtered command to the linear servo-motor for exciting the building. The response quantities in \mathbf{z} are recorded and $\mathbf{H}_{zU}(i\omega)$ is computed through FFT. Then, the mathematical form of $\mathbf{H}_{zU}(s)$ can be obtained by curve-fitting the experimental data to a proper function

$$B(s)/A(s) = (b_n s^n + b_{n-1} s^{n-1} + \dots + b_1 s + b_0) / (s^m + a_{m-1} s^{m-1} + \dots + a_1 s + a_0), n \leq m$$

by using weighted least-square-error method [Wu (2000)]. The resultant curve-fitted amplitude and transfer function \ddot{x}_4 is shown in Fig. 5 (a). The transfer function $\mathbf{H}_{zU}(s)$ can be further converted into the state space equation in time domain expressed by

$$\dot{\mathbf{Z}}_U = \mathbf{A}_U \mathbf{Z}_U + \mathbf{B}_U U; \quad \mathbf{z}_U = \mathbf{C}_U \mathbf{Z}_U + \mathbf{D}_U U \quad (1)$$

in which \mathbf{Z}_U is the state vector; $\mathbf{A}_U, \mathbf{B}_U, \mathbf{C}_U$ and \mathbf{D}_U are constant matrices with appropriate dimensions. Note that the transfer function in this case involves the dynamics introduced by the 2-Hz digital high-pass filter.

In Case 2 where the building is subjected to zero control command ($U=0$) but excited by wind forces (mean wind velocity equal to 8.35m/s), the seven response quantities in \mathbf{z} are recorded. Since the wind forces are not measured as the input source, a normalized (unity spectral density) white noise of fictitious excitation W prior to the actual wind forces is assumed as the input source (see Fig. 3 (a)). Thus, the resulting amplitude of transfer function $\mathbf{H}_{zW}(s)$ can be obtained by directly computing the FFT spectrum of the response. The curve-fitted amplitudes of transfer function \ddot{x}_4 in the cases of along-wind blow ($\alpha=0^\circ$) and across-wind blow ($\alpha=90^\circ$), are shown in Fig. 5 (b) and (c), respectively. By converting to the state space, the state equation in Case 2 is expressed by

$$\dot{\mathbf{Z}}_W = \mathbf{A}_W \mathbf{Z}_W + \mathbf{B}_W W; \quad \mathbf{z}_W = \mathbf{C}_W \mathbf{Z}_W + \mathbf{D}_W W \quad (2)$$

By combining the identification results, Eqs. (1) and (2), in Case 1 and 2, the overall system equation in state space is expressed by

$$\begin{aligned} \dot{\mathbf{Z}} &= \mathbf{A} \mathbf{Z} + \mathbf{B} U + \mathbf{E} W; \\ \mathbf{z} &= \mathbf{z}_U + \mathbf{z}_W = \mathbf{C}_z \mathbf{Z} + \mathbf{D}_z U + \mathbf{F}_z W \end{aligned} \quad (3)$$

in which

$$\mathbf{Z} = \begin{bmatrix} \mathbf{Z}_U \\ \mathbf{Z}_W \end{bmatrix} ; \quad \mathbf{A} = \begin{bmatrix} \mathbf{A}_U & 0 \\ 0 & \mathbf{A}_W \end{bmatrix} ; \quad \mathbf{B} = \begin{bmatrix} \mathbf{B}_U \\ 0 \end{bmatrix} ;$$

$$\mathbf{E} = \begin{bmatrix} 0 \\ \mathbf{B}_W \end{bmatrix} ; \quad \mathbf{C}_z = [\mathbf{C}_U \quad \mathbf{C}_W] ; \quad \mathbf{D}_z = \mathbf{D}_U ; \quad \mathbf{F}_z = \mathbf{D}_W$$

Additionally, the measured output \mathbf{y} used as the feedback quantities can be extracted from \mathbf{z} .

IV. Nominal System And Control Law Design

To truncate the relatively uncontrollable and unobservable states, the overall system identified, Eq. (3), is then further reduced to a minimal realization system using the balanced state reduction method [Moore (1981)]. After reduction, an 18-state reduced-order system is constructed as the nominal system for the control law design. For demonstration of the feasibility of the system identification scheme proposed to wind-excited buildings, the well-known control strategy, linear quadratic gaussian (LQG) method which is also used as a sample in the benchmark problem [Spencer et al. (1998), Yang and Wu et al (1998)], is used for the control law design. The brief explanation and summary of LQG theory can be found in [Wu et al (2000)]. Consequently, the computation of the LQG control command U can be obtained by a dynamic output feedback equation. For implementation in the tests, this dynamic output feedback controller is further discretized into a discrete form using bilinear transformation [Paraskevopoulos (1996)] with a sampling interval of 0.001 sec.

V. Experimental Results

Boundary layer wind Tunnel tests of the high-rise building model are conducted using LQG control under three different mean wind velocity of 7.13, 8.35 and 8.86 m/sec. These velocities are equivalent to the reference wind velocities (at 10 m height) of 19.4, 22.7 and 24.1 m/sec, respectively, in the suburban area. Five attack angles of wind are varied to investigate the performance of active control, i.e., $\alpha=0^\circ, 30^\circ, 45^\circ, 70^\circ, 90^\circ$. It is observed that the vortex shedding appears as α is larger than 65° . Therefore, the LQG controller designed based on the nominal system of $\alpha=0^\circ$ (along-wind) is used for the cases $\alpha=0^\circ, 30^\circ, 45^\circ$, while that based on the nominal system of $\alpha=90^\circ$ (across-wind) is used for the cases $\alpha=70^\circ$ and 90° . The plot of experimental displacement and acceleration of the 4th DOF in temporal root-mean-square (rms) values are presented in Fig.6 as function of attack angles. In Fig.6, the upper half illustrates the rms displacement and the reduction percentage w.r.t. no control case, while the bottom half illustrates the rms acceleration and the reduction percentage. As shown in Fig.6, the performance of LQG control can achieve 35% to 60% in reducing rms

displacement and acceleration, depending on the attack angle.

VI. Conclusions

Wind tunnel tests using a four-degree-of-freedom high-rise building model have been successfully conducted to verify the applicability of a feasible design process proposed for active control. The aeroelasticity induced by the vortex shedding effect is taken into account in the identification scheme. The experimental results show that the performance of the active controller following the design process is remarkable and robust under different attack angle of wind.

VII. References

1. Kabori, T., Inoue, Y., Seto, K., Iemura, H. and Nishitani, A. (editors) (1998), Proceedings of Second World Conference on Structural Control, John Wiley & Sons, N. Y.
2. Housner, G. W., Masri, S. F. and Chassiakos, A. G. (editors) (1994) *Proceedings of First World Conference on Structural Control*, USC, LA.
3. Kabori, T., Inoue, Y., Seto, K., Iemura, H. and Nishitani, A. (editors) (1998) *Proceedings of Second World Conference on Structural Control*, John Wiley & Sons, N. Y.
4. Moore, B. C. (1981) Principal Component Analysis in Linear System: Controllability, Observability and Model Reduction. *IEEE Transactions on Automatic Control*, Vol. 26, No. 1, pp. 17-32.
5. Paraskevopoulos P. N. (1996) *Digital Control Systems*, Prentice Hall, NJ.
6. Simiu, E. and Scanlan, R. H. (1996) *Wind Effects on Structures*, John Wiley, NY.
7. Spencer, B.F. Jr., Dyke, S.J. and Deoskar, H.S. (1998) Benchmark Problems in Structural Control - Part I: Active Mass Driver System. Part II: Active Tendon System. *Earthq. Eng. and Struct. Dyn.*, Vol. 27, pp. 1127-1147.
8. Wu, J. C. (2000) Modeling of an Actively Braced Full-Scale Building Considering Control-Structure Interaction. *Earthq. Eng. and Struct. Dyn.*, Vol. 29, No. 9, Sep., pp. 1325-1342.
9. Wu, J. C. and Pan, B. C. (2001) Wind Tunnel Verification of Active Control for High-rise Building, *Proc. of 5th Asia-Pacific Conference on Wind Engineering*, pp. 441-444, Kyoto, Japan.
10. Yang, J.N., Wu, J.C., Samali, B. and Agrawal, A.K. (1998) A Benchmark Problem for Response Control of Wind-Excited Tall Buildings. *Proc. 2nd World Conference on Structural Control*, Vol.2, pp. 1407-1416, John Wiley & Sons, New York.

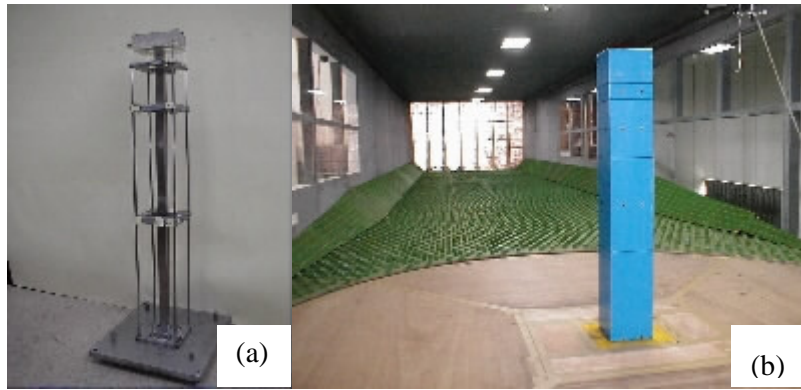


Fig.1: (a) Frame Skeleton of the 1:300 Scaled High-rise Building Model; (b) The Completed Building Model on the Boundary Layer Wind Tunnel

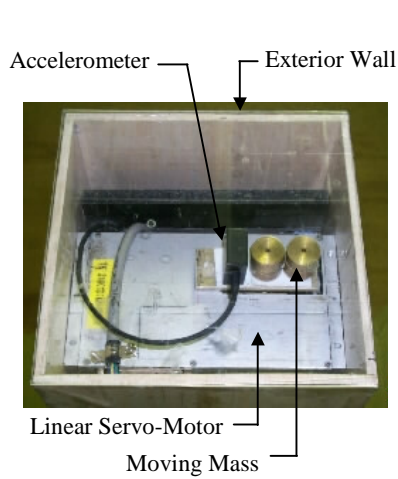


Fig.2: Active Mass Driver System on the Top Floor

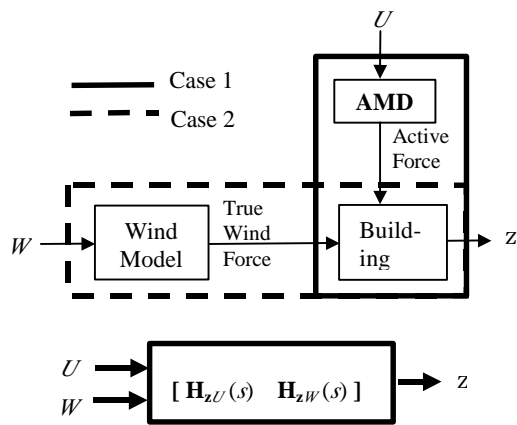


Fig.3: (a) Schematic Block Diagram of the Overall Integrated System; (b) Block Diagram in Laplace Domain.

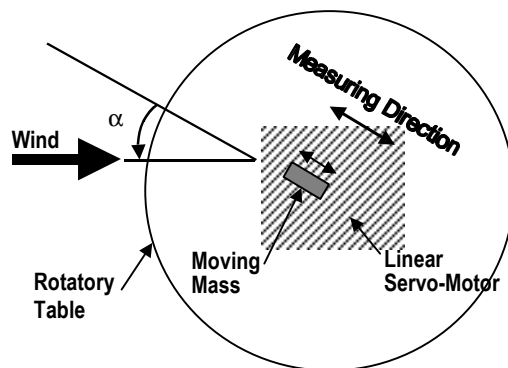


Fig. 4: Configuration of Attack Angle of Wind in the Wind Tunnel

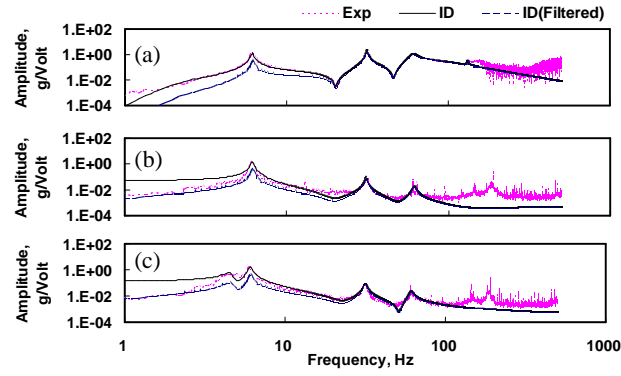


Fig.5: Amplitude of Transfer Function \ddot{x}_4 : (a) due to Actuator Command U ; (b) due to Along-wind Fictitious Load W ; (c) due to Across-Wind Fictitious Load W

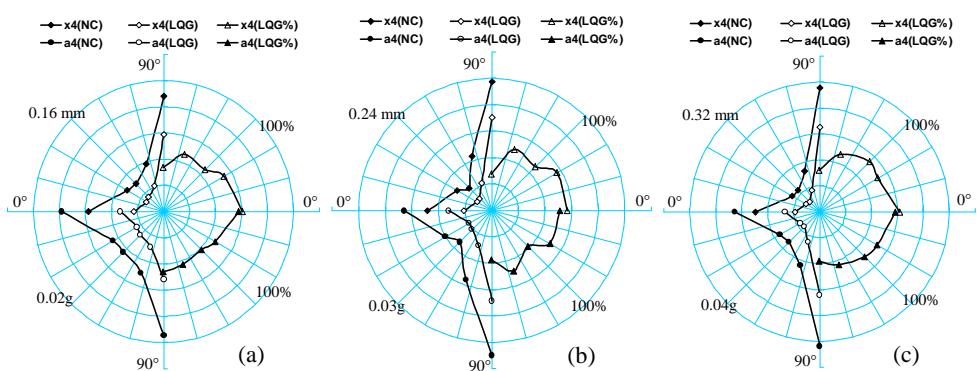


Fig. 6: Performance Diagram of Active Control under Different Attack Angle of Wind
 (a) Wind Speed=7.13 m/s; (b) Wind Speed=8.35 m/s; (c) Wind Speed=8.86 m/s

